



Hierarchical closed form solutions for plates bent by localized transverse loadings

CARRERA E., GIUNTA G., BRISCHETTO S.

(Aeronautical and Space Department, Politecnico di Torino, c.so Duca degli Abruzzi, 24, 10129 Torino, Italy)

E-mail: erasmo.carrera@polito.it; gaetano.giunta@polito.it; salvatore.brischetto@polito.it

Received Feb. 12, 2007; revision accepted May 8, 2007

Abstract: 3D and 2D closed form plate models are here applied to static analysis of simply supported square isotropic plates. 2D theories are hierarchically classified on the basis of the accuracy of the displacements and stresses obtained by comparison to the 3D exact results that could be assumed by the reader as benchmark for further analyses. Attention is mainly paid on localized loading conditions, that is, piecewise constant load. Also bi-sinusoidal and uniformly distributed loadings are taken into account. All of those configurations are considered in order to investigate the behavior of the 2D models in the case of continuous/uncontinuous, centric or off-centric loading conditions. The ratio between the side length a and the plate thickness h has been assumed as analysis parameter. Higher order 2D models yield accurate results for any considered load condition in the case of moderately thick plates, $a/h=10$. In the case of thick plates, $a/h=5$, and continuous/uncontinuous centric loading conditions high accuracy is also obtained. For the considered off-centric load condition and thick plates good results are provided for some output quantities. A better solution could be achieved by simply increasing the polynomial approximation order of the axiomatic 2D displacement field.

Key words: Exact 3D model, Hierarchical 2D models, Principle of Virtual Displacements (PVD), Localized loading, Simply supported square isotropic plate

doi:10.1631/jzus.2007.A1026

Document code: A

CLC number: TU2; TU3

INTRODUCTION

Bending analysis of plates has occupied and still assumes a relevant role in the mechanics of structures from the engineering and mathematical points of view. Cases where localized loading conditions are taken into account represent an interesting problem class since they involve more general and complex loadings and are representative of closer to the reality conditions. On this aspect works (Meyer-Piening, 2000; Anderson *et al.*, 1998; Barut *et al.*, 2000; Carrera and Demasi, 2003; Carrera and Ciuffreda, 2005) can be mentioned. In this work static analyses of simply supported isotropic plates are addressed. In the theoretical environment of closed form solutions, displacement and stress fields are:

$$\left\{ \begin{array}{l} (u(x, y, z), \sigma_{xz}(x, y, z)) \\ = \sum_{m=1}^M \sum_{n=1}^N (U(z), S_{xz}(z)) \cos\left(\frac{m\pi}{a}x\right) \sin\left(\frac{n\pi}{b}y\right), \\ (v(x, y, z), \sigma_{yz}(x, y, z)) \\ = \sum_{m=1}^M \sum_{n=1}^N (V(z), S_{yz}(z)) \sin\left(\frac{m\pi}{a}x\right) \cos\left(\frac{n\pi}{b}y\right), \\ (w(x, y, z), \sigma_{zz}(x, y, z)) \\ = \sum_{m=1}^M \sum_{n=1}^N (W(z), S_{zz}(z)) \sin\left(\frac{m\pi}{a}x\right) \sin\left(\frac{n\pi}{b}y\right), \\ (\sigma_{xx}(x, y, z), \sigma_{yy}(x, y, z)) \\ = \sum_{m=1}^M \sum_{n=1}^N (S_{xx}(z), S_{yy}(z)) \sin\left(\frac{m\pi}{a}x\right) \sin\left(\frac{n\pi}{b}y\right), \\ \sigma_{xy}(x, y, z) = \sum_{m=1}^M \sum_{n=1}^N S_{xy}(z) \cos\left(\frac{m\pi}{a}x\right) \cos\left(\frac{n\pi}{b}y\right). \end{array} \right. \quad (1)$$

Unknown amplitudes in the previous equations are calculated by means of the 3D model in (Demasi, 2007), briefly presented in Section 2, and via some 2D displacements based models, reported in Section 3 where a 2D plate model unifying and hierarchically classifying environment is assumed. Several loadings conditions are analyzed by means of Fourier's series approximations in Section 4. Continuous loading conditions are assumed in subsections 4.1 and 4.2, where bi-sinusoidal and uniformly distributed loads are taken into account. Contribution to the research field is provided in subsections 4.3 and 4.4 where attention is focused on centric and off-centric step-wise constant loadings. Analyses are performed considering the ratio between the plate length side a and thickness h as parameters in order to deal with thin and thick plates. Attention is focused on displacements and stresses computation and comparison from a local point of view, punctual values, and from a global point of view: along the plate thickness or along an in-plane coordinate. Reference system is a Cartesian one. It has its origin at one plate corner: x and y axes are along the plate sides, z identifies along the thickness direction such as $0 \leq x \leq a$, $0 \leq y \leq b$ and $-h/2 \leq z \leq h/2$.

3D SOLUTION

There exist several 3D plates exact solutions; (Levinson, 1985; Barrett and Ellis, 1988; Pagano, 1969; Pagano, 1970) represent an example of the wide literature on the topic. The solution assumed in this paper for isotropic simply supported plates has been taken from (Demasi, 2007). Here only a brief explanation is reported, for more details, refer to the above cited work. There a Navier type exact solution has been obtained via integration of a system of six first order differential equations whose variables are the displacement amplitudes (U, V, W) and the out-of-plane stress amplitudes (S_{zz}, S_{xz}, S_{yz}) . Solution of that system ensures that in any point of the plate Hook's equation, displacements-strain geometric relations and indefinite equilibrium equations are satisfied. If only a bi-sinusoidal load acts on the plate's top, a closed form solution for displacements and stress amplitudes can be obtained. Those quantities are function of the number of half waves (m, n) , plate geometry, load amplitude, plate material and

along thickness coordinate. Here new analyses are presented where several loading conditions are taken into account: bi-sinusoidal loads in subsection 4.1, uniform load in subsection 4.2 and localized centric and off-centric loadings in subsections 4.3 and 4.4.

HIERARCHICAL 2D SOLUTION

In literature a wide variety of 2D closed form solutions are present. Works (Timoshenko and Woinowsky-Krieger, 1959; Love, 1944; Reddy, 1997; He, 1995; Zenkour, 2003; Carrera, 2002; 2003) provide an idea of the several proposed theories. In particular taking place from (Carrera, 2002) a unifying theoretical environment, here adopted, has been proposed in (Carrera, 2003) for the general case of multilayered, anisotropic, composite plates and shells. In such a general theoretical environment a broad variety of plate models, based on an axiomatic approach, can be hierarchically classified and compared on the basis of: (1) polynomial expansion order along the thickness; (2) variational statement; (3) laminate or lamina description level.

In this work all of the theories that are based on the axiomatic displacements field shown in Eq.(2) are applied and compared.

$$(U(z), V(z)) = \sum_{i=0}^{N_u} z^i (U_i, V_i), \quad W(z) = \sum_{j=0}^{N_w} z^j W_j. \quad (2)$$

Displacements amplitudes in Eq.(2) are approximated via McLaurin's series expansion with respect to z coordinate. In this way the polynomials coefficients (U_i, V_i, W_j) ($i=1, \dots, N_u; j=1, \dots, N_w$) become the new problem unknowns. They are computed by means of the Principle of Virtual Displacements (PVD):

$$\int_V (\delta \{\boldsymbol{\varepsilon}_{pG}\}^T \{\boldsymbol{\sigma}_{pC}\} + \delta \{\boldsymbol{\varepsilon}_{nG}\}^T \{\boldsymbol{\sigma}_{nC}\}) dV = \delta L_e. \quad (3)$$

where subscripts 'p' and 'n' represent the in-plane and out-of-plane stress/strain components respectively; subscript 'G' means that strain components have been obtained by means of derivation of the displacement field and 'C' stands for stress components computed via the material constitutive equa-

tions (Hook's generalized law). Several classical and higher order plate models can be easily obtained from Eq.(2). Choosing $N_u=1$ and $N_w=0$, the displacement field consistent with the first order shear deformation theory (FSDT) is obtained. In order to mention higher order theories the acronym system adopted in (Carrera, 2003) is here assumed. That acronym is composed of two letters and a number. The first letter is 'E' and it indicates that all of the considered theories are members of the general class of 'equivalent single layer' theories. It seems to be a tautology in the case of isotropic plate but it is an inheritance from the broader and more general theories in (Carrera, 2003). The second letter represents the assumed variation statement and for Eq.(3) or equivalently for Eq.(2) it is 'D' standing for displacements based problem. The number represents the polynomial order in Eq.(2). For example an ED3 theory is a displacement based model where displacement amplitudes are approximated via cubic polynomial functions:

$$(U(z), V(z), W(z)) = (U_0, V_0, W_0) + (U_1, V_1, W_1)z + (U_2, V_2, W_2)z^2 + (U_3, V_3, W_3)z^3. \quad (4)$$

A peculiarity of higher order theories is that due to their formulation the shear correction factor is not required; σ_{xz} and σ_{yz} stress components can be approximated via a high order polynomial function. Transverse and shear deformations are considered in the models. Also, out-of-plane stresses satisfy with high accuracy the boundary conditions at plate top and bottom. Considerations and results probing and proving the above addressed points can be found in (Carrera and Demasi, 2003; Carrera and Ciuffreda, 2005; Carrera, 2003).

In this work the maximum polynomials expansion order is considered to be four.

CASE STUDY

In this section analyses of plates for different loading conditions are presented. In all of the cases plates have the same geometry and are made of the same isotropic material: aluminum alloy 7075-T651. Thickness ratio a/h has been chosen as analysis parameter in order to determine the applicability threshold of the 2D plate models. Geometrical data

are: $a=300$ mm; $b=300$ mm; $a/h=100,50,10,5,2$. The material mechanical properties are: Poisson's ratio $\nu=0.33$; Young's modulus $E=71700$ N/mm². In all of the loading cases an amplitude equal to one is considered.

Due to the problem linearity a generic load can be expressed by means of its Fourier's series approximation Eq.(5):

$$q_z \approx \sum_{m=1}^M \sum_{n=1}^N q_{mn} \sin\left(\frac{m\pi}{a}x\right) \sin\left(\frac{n\pi}{b}y\right), \quad (5)$$

where coefficients q_{mn} depend on the particular loading condition that has been taken into account. M and N are the number of the considered harmonic terms in x and y directions respectively. The original problem is, thus, split into $M \times N$ problems characterized by a bi-sinusoidal loading and its solution is the superposition of all of the $M \times N$ solutions of the harmonic problems. In subsection 4.1 some bi-sinusoidal loading conditions are taken into account in order to show the level of approximation provided by the 2D plate models for some elements of the Fourier's series expansion. In subsections 4.2 to 4.4 distributed loadings acting on the whole plate or on a part of it are presented. Analogous work had been done in (Carrera and Demasi, 2003; Carrera and Ciuffreda, 2005) in the case of laminated plates. Analyses are computed assuming 3D and 2D plates models. A hierarchy among the 2D closed form plate theories is established by means of comparison of their results to those obtained via the exact 3D solution.

Plate subjected to bi-sinusoidal loadings

Since a generic loading condition can be expressed as a sum of harmonic components via its Fourier's series approximation, in this subsection, a plate subjected to several bi-sinusoidal loadings is considered. Analyses are performed varying the half waves numbers in x and y directions (m, n) and the ratio a/h . Attention is focused on displacement amplitudes (U, V, W) and in-plane stress amplitudes (S_{xx}, S_{xy}), computed at plate top. Also S_{zz} amplitude, evaluated at plate middle point, is taken into account. Results computed via exact 3D model are taken as reference in order to compare what was obtained via all of the considered 2D models. In Tables 1 and 2 displacement and stress amplitudes are reported in the

Table 1 Displacement amplitudes (U, V, W) at plate top (mm), $a/h=100$

(m,n)	U, V, W				
	3D	FSDT	ED2	ED3	ED4
(1,1)	-1.8036	-1.8037	-1.8034	-1.8036	-1.8036
	-1.8036	-1.8037	-1.8034	-1.8036	-1.8036
	1.1487×10^2	1.1489×10^2	1.1487×10^2	1.1487×10^2	1.1487×10^2
(1,10)	-7.0389×10^{-4}	-7.0727×10^{-4}	-7.0144×10^{-4}	-7.0389×10^{-4}	-7.0389×10^{-4}
	-7.0389×10^{-3}	-7.0727×10^{-3}	-7.0144×10^{-3}	-7.0389×10^{-3}	-7.0389×10^{-3}
	4.5938×10^{-2}	4.6143×10^{-2}	4.5781×10^{-2}	4.5937×10^{-2}	4.5938×10^{-2}
(10,10)	-1.7869×10^{-3}	-1.8037×10^{-3}	-1.7745×10^{-3}	-1.7869×10^{-3}	-1.7869×10^{-3}
	-1.7869×10^{-3}	-1.8037×10^{-3}	-1.7745×10^{-3}	-1.7869×10^{-3}	-1.7869×10^{-3}
	1.1950×10^{-2}	1.2047×10^{-2}	1.1870×10^{-2}	1.1950×10^{-2}	1.1950×10^{-2}
(1,50)	-1.0682×10^{-6}	-1.1535×10^{-6}	-9.6023×10^{-7}	-1.0639×10^{-6}	-1.0682×10^{-6}
	-5.3412×10^{-5}	-5.7673×10^{-5}	-4.8011×10^{-5}	-5.3193×10^{-5}	-5.3410×10^{-5}
	1.2320×10^{-4}	1.1852×10^{-4}	1.1590×10^{-4}	1.2291×10^{-4}	1.2320×10^{-4}
(50,50)	-1.3425×10^{-5}	-1.4430×10^{-5}	-1.0447×10^{-5}	-1.3196×10^{-5}	-1.3419×10^{-5}
	-1.3425×10^{-5}	-1.4430×10^{-5}	-1.0447×10^{-5}	-1.3196×10^{-5}	-1.3419×10^{-5}
	4.9798×10^{-5}	4.0926×10^{-5}	4.5604×10^{-5}	4.9490×10^{-5}	4.9789×10^{-5}

Table 2 S_{xx}, S_{xy} at plate top and S_{zz} at plate middle point (N/mm^2), $a/h=100$

(m,n)	$S_{xx}, S_{xy}, S_{zz}, S_{zz}^*$				
	3D	FSDT	ED2	ED3	ED4
(1,1)	2.0217×10^3	2.0214×10^3	2.0215×10^3	2.0218×10^3	2.0217×10^3
	-1.0182×10^3	-1.0183×10^3	-1.0181×10^3	-1.0182×10^3	-1.0182×10^3
	5.0000×10^{-1}	5.0000×10^{-1}	5.0000×10^{-1}	5.0000×10^{-1}	5.0000×10^{-1}
(1,10)	-	-	$4.9997 \times 10^{-1*}$	$5.0000 \times 10^{-1*}$	$5.0000 \times 10^{-1*}$
	2.0658×10^1	2.0262×10^1	2.0597×10^1	2.0787×10^1	2.0658×10^1
	-3.9738	-3.9929	-3.9599	-3.9738	-3.9738
(10,10)	4.9999×10^{-1}	5.0000×10^{-1}	4.9999×10^{-1}	4.9999×10^{-1}	4.9999×10^{-1}
	-	-	$4.9865 \times 10^{-1*}$	$4.9999 \times 10^{-1*}$	$4.9999 \times 10^{-1*}$
	2.0518×10^1	2.0214×10^1	2.0389×10^1	2.0647×10^1	2.0518×10^1
(1,50)	-1.0088×10^1	-1.0183×10^1	-1.0018×10^1	-1.0088×10^1	-1.0088×10^1
	4.9995×10^{-1}	5.000×10^{-1}	4.9995×10^{-1}	4.9996×10^{-1}	4.9995×10^{-1}
	-	-	$4.9732 \times 10^{-1*}$	$4.9996 \times 10^{-1*}$	$4.9996 \times 10^{-1*}$
(50,50)	1.2360	8.0279×10^{-1}	1.1912	1.3614	1.2383
	-3.0153×10^{-2}	-3.2559×10^{-2}	-2.7104×10^{-2}	-3.0030×10^{-2}	-3.0152×10^{-2}
	4.9301×10^{-1}	5.0000×10^{-1}	4.9286×10^{-1}	4.9397×10^{-1}	4.9301×10^{-1}
(50,50)	-	-	$4.6674 \times 10^{-1*}$	$4.9406 \times 10^{-1*}$	$4.9456 \times 10^{-1*}$
	1.2448	8.0854×10^{-1}	1.1193	1.3593	1.2521
	-3.7896×10^{-1}	-4.0731×10^{-1}	-2.9489×10^{-1}	-3.7247×10^{-1}	-3.7878×10^{-1}
(50,50)	4.7553×10^{-1}	5.0000×10^{-1}	4.7553×10^{-1}	4.7820×10^{-1}	4.7548×10^{-1}
	-	-	$4.3485 \times 10^{-1*}$	$4.7851 \times 10^{-1*}$	$4.8082 \times 10^{-1*}$

S_{zz}^* : computed via constitutive equations

case of a thin plate, $a/h=100$, and $(m,n)=(1,1),(1,10),(10,10),(1,50),(50,50)$. Terms S_{zz}^* are computed by means of constitutive equations, S_{zz} by integration of indefinite equilibrium equations. A first consideration can be already addressed: increasing m and n , even in the case of thin plates, as results obtained via FSDT and ED2 can be affected by relevant errors. For $(m,n)=(1,50),(50,50)$ the absolute percentage error for U and V can be above 8% (FSDT) and 10% (ED2), while ED3 provides results affected by an approximation lower than 1.8% and ED4 can be practically considered to coincide with the exact 3D solution.

Since stress amplitudes are not directly furnished by the mathematical models but obtained via a post processing of the displacements, less accurate results are expected. EDN models describe S_{zz} with a high accuracy even via the constitutive equations. That result is relevant considering that S_{zz} is not anymore negligible; when $(m,n)=(1,50),(50,50)$, $S_{zz}/S_{xx} \approx 0.4$. S_{xx} is affected by relevant approximation being the absolute percentage error of about 35% for FSDT and 10% for ED3. A fourth order polynomial approximation ensures high accuracy, being the absolute percentage error lower than 0.6%. Tables 3 and 4 report

results related to a thick plate, $a/h=2$. For small numbers of half waves $(m,n)=(1,4),(4,4)$, even higher order 2D models provide results affected by high approximation. This behavior is due to the fact that increasing (m,n) along the thickness only a smaller and smaller part of the plate is subjected to a non zero stress-strain state since loading assumes practically only minima and maxima that are equal in modulus. The phenomenon is made more obvious by small values of a/h . Figs.1 and 2 show the maximum value of (m,n) for displacement amplitudes U, V and W made by varying the plate thickness and for a

percentage error threshold of about 2% and 5% respectively. Since a square plate under symmetric material constraints and loadings ($m=n$) conditions are considered, displacement amplitudes U and V are equal. Shown results underline the existence of a hierarchy, in terms of results quality, of the considered 2D plate models. At this point it is important to state that for a general loading condition the contribution of every single harmonic term to the global solution is weighted by the corresponding part of the global loading computed via its Fourier's series approximation Eq.(5). How it will show in the next

Table 3 Displacement amplitudes (U,V,W) at plate top (mm), $a/h=2$

(m,n)	U,V,W				
	3D	FSDT	ED2	ED3	ED4
(1,1)	-6.7126×10^{-4}	-7.2149×10^{-4}	-5.2235×10^{-4}	-6.5978×10^{-4}	-6.7095×10^{-4}
	-6.7126×10^{-4}	-7.2149×10^{-4}	-5.2235×10^{-4}	-6.5978×10^{-4}	-6.7095×10^{-4}
	2.4899×10^{-3}	2.0493×10^{-3}	2.2802×10^{-3}	2.4745×10^{-3}	2.4894×10^{-3}
(1,2)	-1.4229×10^{-4}	-1.1544×10^{-4}	-6.6694×10^{-5}	-1.2813×10^{-4}	-1.4110×10^{-4}
	-2.8458×10^{-4}	-2.3088×10^{-4}	-1.3339×10^{-4}	-2.5626×10^{-4}	-2.8219×10^{-4}
	1.1262×10^{-3}	5.9805×10^{-3}	1.0056×10^{-3}	1.1045×10^{-3}	1.1241×10^{-3}
(2,2)	-1.5712×10^{-4}	-9.0186×10^{-5}	-4.7512×10^{-5}	-1.2434×10^{-4}	-1.5247×10^{-4}
	-1.5712×10^{-4}	-9.0186×10^{-5}	-4.7512×10^{-5}	-1.2434×10^{-4}	-1.5247×10^{-4}
	8.5079×10^{-4}	3.3933×10^{-4}	7.4955×10^{-4}	8.2109×10^{-4}	8.4596×10^{-4}
(1,4)	-3.5482×10^{-5}	-9.9860×10^{-6}	-3.8251×10^{-6}	-1.7980×10^{-5}	-3.0412×10^{-5}
	-1.4193×10^{-4}	-3.9944×10^{-5}	-1.5300×10^{-5}	-7.1920×10^{-5}	-1.2165×10^{-4}
	5.7595×10^{-4}	1.4538×10^{-4}	4.8588×10^{-4}	5.3135×10^{-4}	5.6156×10^{-4}
(4,4)	-7.5284×10^{-5}	-1.1273×10^{-5}	2.2730×10^{-6}	-1.8353×10^{-5}	-4.8349×10^{-5}
	-7.5284×10^{-5}	-1.1273×10^{-5}	2.2730×10^{-6}	-1.8353×10^{-5}	-4.8349×10^{-5}
	4.1960×10^{-4}	7.4068×10^{-5}	3.2913×10^{-4}	3.6971×10^{-4}	3.9470×10^{-4}

Table 4 S_{xx}, S_{xy} at plate top and S_{zz} at plate middle point (N/mm^2), $a/h=2$

(m,n)	$S_{xx}, S_{xy}, S_{zz}, S_{zz}^*$				
	3D	FSDT	ED2	ED3	ED4
(1,1)	1.2448	8.0854×10^{-1}	1.1193	1.3593	1.2521
	-3.7896×10^{-1}	-4.0731×10^{-1}	-2.9489×10^{-1}	-3.7247×10^{-1}	-3.7878×10^{-1}
	4.7553×10^{-1}	5.0000×10^{-1}	4.7553×10^{-1}	4.7820×10^{-1}	4.7548×10^{-1}
(1,2)	—	—	$4.3485 \times 10^{-1*}$	$4.7851 \times 10^{-1*}$	$4.8082 \times 10^{-1*}$
	7.7069×10^{-1}	2.2566×10^{-1}	6.6055×10^{-1}	8.6498×10^{-1}	7.9855×10^{-1}
	-1.6065×10^{-1}	-1.3034×10^{-1}	-7.5303×10^{-2}	-1.4467×10^{-1}	-1.5931×10^{-1}
(2,2)	3.9705×10^{-1}	5.0000×10^{-1}	3.9982×10^{-1}	4.0241×10^{-1}	3.9600×10^{-1}
	—	—	$3.5322 \times 10^{-1*}$	$4.0337 \times 10^{-1*}$	$4.1770 \times 10^{-1*}$
	8.4469×10^{-1}	2.0214×10^{-1}	6.1095×10^{-1}	8.8492×10^{-1}	8.8565×10^{-1}
(1,4)	-1.7740×10^{-1}	-1.0183×10^{-1}	-5.3645×10^{-2}	-1.4039×10^{-1}	-1.7215×10^{-1}
	3.1777×10^{-1}	5.000×10^{-1}	3.2203×10^{-1}	3.2170×10^{-1}	3.1428×10^{-1}
	—	—	$2.9254 \times 10^{-1*}$	$3.2269 \times 10^{-1*}$	$3.5141 \times 10^{-1*}$
(4,4)	6.8029×10^{-1}	5.2841×10^{-2}	4.3901×10^{-1}	6.6803×10^{-1}	7.3867×10^{-1}
	-8.0125×10^{-2}	-2.2550×10^{-2}	-8.6377×10^{-3}	-4.0602×10^{-2}	-6.8674×10^{-2}
	1.6316×10^{-1}	5.0000×10^{-1}	1.5341×10^{-1}	1.6134×10^{-1}	1.5060×10^{-1}
(4,4)	—	—	$1.8754 \times 10^{-1*}$	$1.5902 \times 10^{-1*}$	$2.1218 \times 10^{-1*}$
	8.3001×10^{-1}	5.0534×10^{-2}	3.2263×10^{-1}	5.9734×10^{-1}	7.9848×10^{-1}
	-1.7000×10^{-1}	-2.5457×10^{-2}	1.0459×10^{-4}	-4.1444×10^{-2}	-1.0918×10^{-1}
	6.3868×10^{-2}	5.0000×10^{-1}	1.3351×10^{-2}	6.0365×10^{-2}	4.2589×10^{-2}
	—	—	$1.1485 \times 10^{-1*}$	$4.8764 \times 10^{-2*}$	$1.0779 \times 10^{-1*}$

S_{zz}^* : computed via constitutive equations

cases, highly approximated results via 2D models can be reached even when a high number of harmonic attributes are taken into account.

Uniform loading

A unitary uniform loading acting on the plate top (Fig.3) is considered. Hence, the plate configuration is symmetric and continuous boundary conditions for displacement and loading are fixed. Analysis has been performed with varying parameters of $a/h \in \{100, 50, 10, 5, 2\}$, in order to investigate the accuracy of the results obtained via 2D hierarchical plate models in the cases of thick and thin plates. Exact 3D solution is taken as reference in order to compare the results. In Table 5 attention is focused on displacements u, v and w computed in correspondence with plate top for the points in the set $D = \{(x,y): x=a/4, 3a/4; y=b/4, 3b/4\}$; due to the problem symmetry those points and displacements u and v are equal. Fourth order 2D theory solution almost matches with exact 3D solution even for very thick plates ($a/h=2$) since the maximum absolute percentage error is about 0.4% for u and v . ED3

model yields the exact solution up to $a/h=5$ (thick plates) and for $a/h=2$, highly accurate results are obtained. Quadratic approximation (ED2) and FSĐT still provide good results for a thick plate, having absolute percentage error of lower than 3.3% and 2.3% respectively. The behavior of u and v along the plate thickness computed by means of the exact 3D model, FSĐT and ED4 for $a/h=5$ is shown in Fig.4. It demonstrates how ED4 solution coincides with the exact one. In Table 6 attention is paid on stresses. In-plane stresses $\{\sigma_{xx}, \sigma_{yy}, \sigma_{xy}\}$ are evaluated in D at plate top. Out-of-plane stresses are computed also in D , but in correspondence with plate middle point; $\{\sigma_{xz}, \sigma_{yz}, \sigma_{zz}\}$ are determined via integration of the indefinite equilibrium equations, while the same stress components marked by superscript, $\{\sigma_{xz}^*, \sigma_{yz}^*, \sigma_{zz}^*\}$, were obtained by means of the constitutive equations. Due to the problem symmetry, $(\sigma_{xx}, \sigma_{yy})$ and $(\sigma_{xz}, \sigma_{yz})$ stresses are equal. Up to $a/h=10$ (moderately thick plates) all of 2D theories yield highly accurate results. For $a/h=5, 2$, ED4 still assures high approximation level, ED3 has the same behavior except for σ_{xx} and

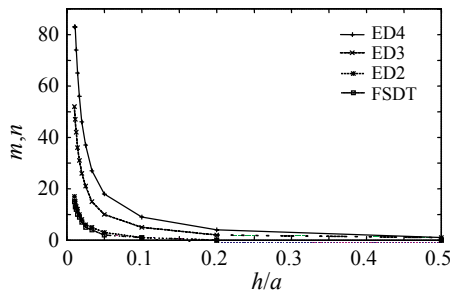


Fig.1 Maxima (m,n) w.r.t $(a/h)^{-1}$ for U and V amplitudes with a percentage error threshold of $\approx 2\%$

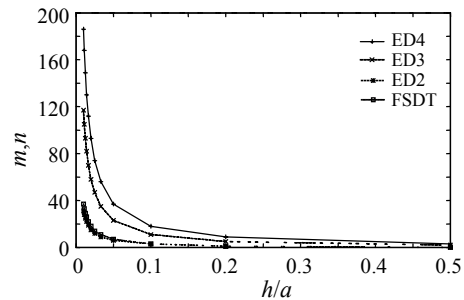


Fig.2 Maxima (m,n) w.r.t $(a/h)^{-1}$ for W amplitudes with a percentage error threshold of $\approx 5\%$

Table 5 Displacements u, v and w at $D = \{(x,y): x=a/4, 3a/4; y=b/4, 3b/4\}$ top for uniform load (mm)

a/h	u, v, w				
	3D	FSĐT	ED2	ED3	ED4
100	-1.4095	-1.4096	-1.4094	-1.4095	-1.4095
	-1.4095	-1.4096	-1.4094	-1.4095	-1.4095
	9.5437×10^1	9.5447×10^1	9.5430×10^1	9.5437×10^1	9.5437×10^1
50	-3.5229×10^{-1}	-3.5240×10^{-1}	-3.5221×10^{-1}	-3.5229×10^{-1}	-3.5229×10^{-1}
	-3.5229×10^{-1}	-3.5240×10^{-1}	-3.5221×10^{-1}	-3.5229×10^{-1}	-3.5229×10^{-1}
	1.1945×10^1	1.1950×10^1	1.1941×10^1	1.1945×10^1	1.1945×10^1
10	-1.3985×10^{-2}	-1.4096×10^{-2}	-1.3906×10^{-2}	-1.3985×10^{-2}	-1.3985×10^{-2}
	-1.3985×10^{-2}	-1.4096×10^{-2}	-1.3906×10^{-2}	-1.3985×10^{-2}	-1.3985×10^{-2}
	9.9586×10^{-2}	1.0044×10^{-1}	9.8873×10^{-2}	9.9583×10^{-2}	9.9586×10^{-2}
5	-3.4124×10^{-3}	-3.5240×10^{-3}	-3.3340×10^{-3}	-3.4121×10^{-3}	-3.4124×10^{-3}
	-3.4124×10^{-3}	-3.5240×10^{-3}	-3.3340×10^{-3}	-3.4121×10^{-3}	-3.4124×10^{-3}
	1.4225×10^{-2}	1.4445×10^{-2}	1.3854×10^{-2}	1.4220×10^{-2}	1.4225×10^{-2}
2	-4.9224×10^{-4}	-5.6384×10^{-4}	-4.1333×10^{-4}	-5.0031×10^{-4}	-4.9407×10^{-4}
	-4.9224×10^{-4}	-5.6384×10^{-4}	-4.1333×10^{-4}	-5.0031×10^{-4}	-4.9407×10^{-4}
	2.2651×10^{-3}	1.7712×10^{-3}	2.0749×10^{-3}	2.2518×10^{-3}	2.2691×10^{-3}

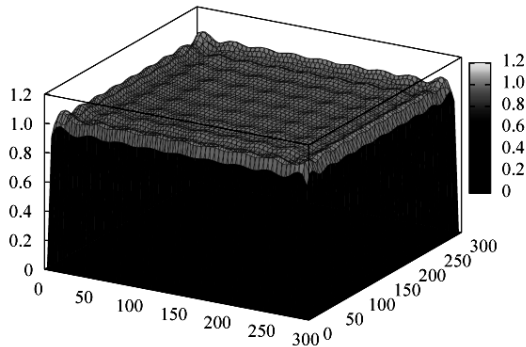


Fig.3 Uniform load via Fourier's series approximations, $M=N=101$

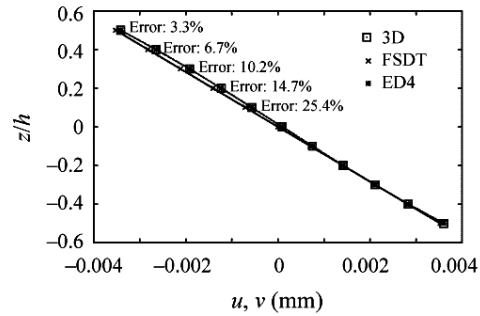


Fig.4 u and v along plate thickness in $(a/4, b/4)$ for uniform load, $a/h=5$

Table 6 In-plane stresses ($\sigma_{xx}, \sigma_{yy}, \sigma_{xy}$) at D top and out-of-plane stresses ($\sigma_{xz}, \sigma_{yz}, \sigma_{zz}$) at D middle point for uniform load (N/mm^2)

al/h	$\sigma_{xx}, \sigma_{yy}, \sigma_{xy}, \sigma_{xz}, \sigma_{yz}, \sigma_{zz}, \sigma_{xz}^*, \sigma_{yz}^*, \sigma_{zz}^*$									
	3D	FSDT	ED2	ED3	ED4					
100	1.8072×10^3	1.8069×10^3	1.8071×10^3	1.8073×10^3	1.8072×10^3					
	1.8072×10^3	1.8069×10^3	1.8071×10^3	1.8073×10^3	1.8072×10^3					
	-7.6659×10^2	-7.6664×10^2	-7.6655×10^2	-7.6659×10^2	-7.6659×10^2					
	1.5290×10^1	1.5289×10^1	1.5289×10^1	1.5290×10^1	1.5290×10^1					
	1.5290×10^1	1.5289×10^1	1.5289×10^1	1.5290×10^1	1.5290×10^1					
	5.0011×10^{-1}	5.0009×10^{-1}	5.0011×10^{-1}	5.0011×10^{-1}	5.0011×10^{-1}					
50	—	—	—	$1.5290 \times 10^*$	$1.5290 \times 10^*$					
	—	—	—	$1.5290 \times 10^*$	$1.5290 \times 10^*$					
	—	—	—	$5.0011 \times 10^{-1*}$	$5.0011 \times 10^{-1*}$					
	4.5203×10^2	4.5173×10^2	4.5190×10^2	4.5216×10^2	4.5203×10^2					
	4.5203×10^2	4.5173×10^2	4.5190×10^2	4.5216×10^2	4.5203×10^2					
	-1.9161×10^2	-1.9166×10^2	-1.9157×10^2	-1.9161×10^2	-1.9161×10^2					
10	7.6456	7.6447	7.6447	7.646	7.646					
	7.6456	7.6447	7.6447	7.646	7.646					
	5.0010×10^{-1}	5.0009×10^{-1}	5.0011×10^{-1}	5.0010×10^{-1}	5.0010×10^{-1}					
	—	—	—	7.6455^*	7.6455^*					
	—	—	—	7.6455^*	7.6455^*					
	—	—	—	$5.0010 \times 10^{-1*}$	$5.0010 \times 10^{-1*}$					
5	1.8367×10^1	1.8069×10^1	1.8237×10^1	1.8496×10^1	1.8367×10^1					
	1.8367×10^1	1.8069×10^1	1.8237×10^1	1.8496×10^1	1.8367×10^1					
	-7.6114	-7.6664	-7.5723	-7.6114	-7.6114					
	1.5294	1.5289	1.5289	1.5302	1.5301					
	1.5294	1.5289	1.5289	1.5302	1.5301					
	4.9996×10^{-1}	5.0009×10^{-1}	4.9996×10^{-1}	4.9996×10^{-1}	4.9995×10^{-1}					
2	—	—	—	1.5297^*	1.5292^*					
	—	—	—	1.5297^*	1.5292^*					
	—	—	—	$4.9996 \times 10^{-1*}$	$4.9997 \times 10^{-1*}$					
	4.8157	4.5173	4.6949	4.9427	4.8125					
	4.8157	4.5173	4.6949	4.9427	4.8125					
	-1.8615	-1.9166	-1.8225	-1.8615	-1.8615					
2	7.6470×10^{-1}	7.6447×10^{-1}	7.6447×10^{-1}	7.6521×10^{-1}	7.6510×10^{-1}					
	7.6470×10^{-1}	7.6447×10^{-1}	7.6447×10^{-1}	7.6521×10^{-1}	7.6510×10^{-1}					
	5.0835×10^{-1}	5.0009×10^{-1}	5.0766×10^{-1}	5.0685×10^{-1}	5.0800×10^{-1}					
	—	—	—	$7.6489 \times 10^{-1*}$	$7.6448 \times 10^{-1*}$					
	—	—	—	$7.6489 \times 10^{-1*}$	$7.6448 \times 10^{-1*}$					
	—	—	—	$5.0662 \times 10^{-1*}$	$5.0600 \times 10^{-1*}$					
2	1.1694	7.2277×10^{-1}	1.0848	1.328	1.1895					
	1.1694	7.2277×10^{-1}	1.0848	1.328	1.1895					
	-2.6385×10^{-1}	-3.0666×10^{-1}	-2.2655×10^{-1}	-2.6653×10^{-1}	-2.6345×10^{-1}					
	3.1251×10^{-1}	3.0579×10^{-1}	3.0579×10^{-1}	3.1021×10^{-1}	3.1566×10^{-1}					
	3.1251×10^{-1}	3.0579×10^{-1}	3.0579×10^{-1}	3.1021×10^{-1}	3.1566×10^{-1}					
	5.0654×10^{-1}	5.0009×10^{-1}	5.1676×10^{-1}	5.1178×10^{-1}	5.1124×10^{-1}					
2	—	—	—	$3.0831 \times 10^{-1*}$	$3.1209 \times 10^{-1*}$					
	—	—	—	$3.0831 \times 10^{-1*}$	$3.1209 \times 10^{-1*}$					
	—	—	—	$5.1359 \times 10^{-1*}$	$5.1317 \times 10^{-1*}$					

$D = \{(x,y): x=a/4, 3a/4; y=b/4, 3b/4\}; (\sigma_{xz}^*, \sigma_{yz}^*, \sigma_{zz}^*):$ computed via constitutive equations

σ_{yy} , where the absolute percentage error is about 2.6% and 13.6% respectively. FSDT predicts out-of-plane stresses with an error lower than 2.2%, while errors of 6.2% and 38.2% affect σ_{xx} and σ_{yy} for thick and very thick plates. In-plane stresses σ_{xx} and σ_{yy} along the plate thickness are shown in Fig.5 for $a/h=5$. Results are evaluated at $x=a/4, y=b/4$ and obtained by exact 3D solution, FSDT and ED4.

Centric localized distributed load

In this subsection the following piecewise constant loading is considered as depicted in Fig.6:

$$\begin{cases} 1, & (x,y) \in \{a/3 \leq x \leq 2a/3, b/3 \leq y \leq 2b/3\}; \\ 0, & \text{elsewhere.} \end{cases} \quad (6)$$

In such a way the plate configuration is symmetric but an uncontinuous loading condition is chosen. Displacements are reported in Table 7. They

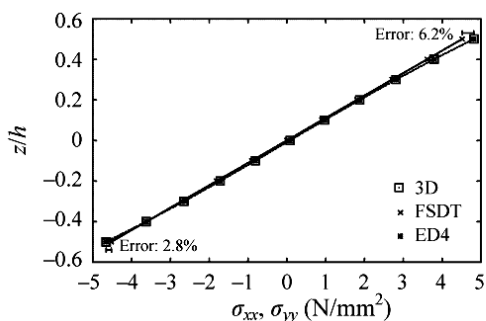


Fig.5 σ_{xx} and σ_{yy} along plate thickness in $(a/4, b/4)$ for uniform load, $a/h=5$

are evaluated in the D set at plate top. The same considerations made in subsection 2 hold, assuming the percentage errors almost the same values. Displacements u and v along the plate thickness via exact 3D solution, FSDT and ED4 are reported in Fig.7, where a very thick plate is considered. As observed in that figure, the results obtained by ED4 agree with the exact solution. The comparison of the stresses is presented in Table 8. Poor correlation against the exact solution for all the stress components for length-to-thickness ratio of $a/h=2$ is observed, which is mainly due to the presence of discontinuous loading. Fig.8 represents the behavior of σ_{xx} and σ_{yy} with respect to the plate z coordinate. Results are obtained by means of exact 3D solution, FSDT and ED4 theories for $a/h=2$. Transverse displacement w at top plate as function of x for $y=b/2$ and $a/h=2$ is plotted in Fig.9. Perfect match is observed between ED4 displacement representation and the exact 3D solution. ED3 representation also yields highly accurate results.

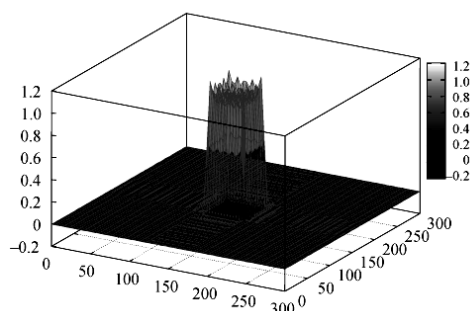


Fig.6 Localized load at $(a/3 \leq x \leq 2a/3, b/3 \leq y \leq 2b/3)$ via Fourier's series approximation, $M=N=61$

Table 7 Displacements u, v and w at D top for localized load at $(a/3 \leq x \leq 2a/3, b/3 \leq y \leq 2b/3)$ (mm)

a/h	u, v, w				
	3D	FSDT	ED2	ED3	ED4
100	-3.7665×10^{-1}	-3.7668×10^{-1}	-3.7662×10^{-1}	-3.7665×10^{-1}	-3.7665×10^{-1}
	-3.7665×10^{-1}	-3.7668×10^{-1}	-3.7662×10^{-1}	-3.7665×10^{-1}	-3.7665×10^{-1}
	2.2125×10^1	2.2127×10^1	2.2124×10^1	2.2125×10^1	2.2125×10^1
50	-9.4134×10^{-2}	-9.4170×10^{-2}	-9.4108×10^{-2}	-9.4134×10^{-2}	-9.4134×10^{-2}
	-9.4134×10^{-2}	-9.4170×10^{-2}	-9.4108×10^{-2}	-9.4134×10^{-2}	-9.4134×10^{-2}
	2.7683	2.7691	2.7677	2.7683	2.7683
10	-3.7305×10^{-3}	-3.7668×10^{-3}	-3.7047×10^{-3}	-3.7304×10^{-3}	-3.7305×10^{-3}
	-3.7305×10^{-3}	-3.7668×10^{-3}	-3.7047×10^{-3}	-3.7304×10^{-3}	-3.7305×10^{-3}
	2.2821×10^{-2}	2.2992×10^{-2}	2.2699×10^{-2}	2.2821×10^{-2}	2.2821×10^{-2}
5	-9.0659×10^{-4}	-9.4170×10^{-4}	-8.8119×10^{-4}	-9.0677×10^{-4}	-9.0655×10^{-4}
	-9.0659×10^{-4}	-9.4170×10^{-4}	-8.8119×10^{-4}	-9.0677×10^{-4}	-9.0655×10^{-4}
	3.1152×10^{-3}	3.2019×10^{-3}	3.0541×10^{-3}	3.1149×10^{-3}	3.1151×10^{-3}
2	-1.3831×10^{-4}	-1.5067×10^{-4}	-1.0879×10^{-4}	-1.3970×10^{-4}	-1.4048×10^{-4}
	-1.3831×10^{-4}	-1.5067×10^{-4}	-1.0879×10^{-4}	-1.3970×10^{-4}	-1.4048×10^{-4}
	3.3370×10^{-4}	3.5181×10^{-4}	3.1095×10^{-4}	3.3684×10^{-4}	3.3423×10^{-4}

$D = \{(x,y): x=a/4, 3a/4; y=b/4, 3b/4\}$

Table 8 In-plane stresses (σ_{xx} , σ_{yy} , σ_{xy}) at D top and out-of-plane stresses (σ_{xz} , σ_{yz} , σ_{zz}) at D middle point for localized load at ($a/3 \leq x \leq 2a/3$, $b/3 \leq y \leq 2b/3$) (N/mm²)

a/h	$\sigma_{xx}, \sigma_{yy}, \sigma_{xy}, \sigma_{xz}, \sigma_{yz}, \sigma_{zz}, \sigma_{xz}^*, \sigma_{yz}^*, \sigma_{zz}^*$				
	3D	FSDT	ED2	ED3	ED4
100	3.1345×10^2	3.1345×10^2	3.1345×10^2	3.1345×10^2	3.1345×10^2
	3.1345×10^2	3.1345×10^2	3.1345×10^2	3.1345×10^2	3.1345×10^2
	-2.4459×10^2	-2.4462×10^2	-2.4456×10^2	-2.4459×10^2	-2.4459×10^2
	4.995	4.995	4.995	4.995	4.995
	4.995	4.995	4.995	4.995	4.995
	2.2422×10^{-4}	2.4708×10^{-4}	2.2452×10^{-4}	2.2625×10^{-4}	2.2412×10^{-4}
	-	-	-	4.995*	4.995*
	-	-	-	4.995*	4.995*
	-	-	-	2.2652×10^{-4}	2.2906×10^{-4}
	-	-	-	-	-
50	7.8363×10^1	7.8363×10^1	7.8363×10^1	7.8363×10^1	7.8363×10^1
	7.8363×10^1	7.8363×10^1	7.8363×10^1	7.8363×10^1	7.8363×10^1
	-6.1120×10^1	-6.1156×10^1	-6.1095×10^1	-6.1120×10^1	-6.1120×10^1
	2.4975	2.4975	2.4975	2.4975	2.4975
	2.4975	2.4975	2.4975	2.4975	2.4975
	1.1745×10^{-4}	2.4708×10^{-4}	1.1818×10^{-4}	1.1790×10^{-4}	1.1381×10^{-4}
	-	-	-	2.4975*	2.4975*
	-	-	-	2.4975*	2.4975*
	-	-	-	1.1797×10^{-4}	1.3913×10^{-4}
	-	-	-	-	-
10	3.1349	3.1345	3.1336	3.1348	3.1349
	3.1349	3.1345	3.1336	3.1348	3.1349
	-2.4105	-2.4462	-2.3853	-2.4103	-2.4104
	4.9950×10^{-1}	4.9950×10^{-1}	4.9950×10^{-1}	4.9949×10^{-1}	4.9948×10^{-1}
	4.9950×10^{-1}	4.9950×10^{-1}	4.9950×10^{-1}	4.9949×10^{-1}	4.9948×10^{-1}
	-7.5053×10^{-4}	2.4708×10^{-4}	-8.1937×10^{-4}	-5.6300×10^{-4}	-6.9020×10^{-4}
	-	-	-	4.9949×10^{-1} *	4.9949×10^{-1} *
	-	-	-	4.9949×10^{-1} *	4.9949×10^{-1} *
	-	-	-	-5.9471×10^{-4} *	-5.4482×10^{-4} *
	-	-	-	-	-
5	7.7519×10^{-1}	7.8363×10^{-1}	7.6862×10^{-1}	7.7246×10^{-1}	7.7572×10^{-1}
	7.7519×10^{-1}	7.8363×10^{-1}	7.6862×10^{-1}	7.7246×10^{-1}	7.7572×10^{-1}
	-5.8189×10^{-1}	-6.1156×10^{-1}	-5.5674×10^{-1}	-5.8318×10^{-1}	-5.8206×10^{-1}
	2.5031×10^{-1}	2.4975×10^{-1}	2.4975×10^{-1}	2.5007×10^{-1}	2.5026×10^{-1}
	2.5031×10^{-1}	2.4975×10^{-1}	2.4975×10^{-1}	2.5007×10^{-1}	2.5026×10^{-1}
	-4.8635×10^{-3}	2.4708×10^{-4}	-4.7505×10^{-3}	-5.2354×10^{-3}	-5.0587×10^{-3}
	-	-	-	2.4993×10^{-1} *	2.5012×10^{-1} *
	-	-	-	2.4993×10^{-1} *	2.5012×10^{-1} *
	-	-	-	-5.3070×10^{-3} *	-4.1848×10^{-3} *
	-	-	-	-	-
2	8.2769×10^{-2}	1.2538×10^{-2}	9.9056×10^{-2}	8.9075×10^{-2}	6.7206×10^{-2}
	8.2769×10^{-2}	1.2538×10^{-2}	9.9056×10^{-2}	8.9075×10^{-2}	6.7206×10^{-2}
	-1.0491×10^{-1}	-9.7849×10^{-2}	-6.8089×10^{-2}	-1.0041×10^{-1}	-1.0863×10^{-1}
	1.0047×10^{-1}	9.9900×10^{-2}	9.9900×10^{-2}	1.0083×10^{-1}	1.0388×10^{-1}
	1.0047×10^{-1}	9.9900×10^{-2}	9.9900×10^{-2}	1.0083×10^{-1}	1.0388×10^{-1}
	3.1452×10^{-2}	2.4708×10^{-4}	2.6741×10^{-2}	3.1460×10^{-2}	3.2158×10^{-4}
	-	-	-	1.0043×10^{-1} *	1.0186×10^{-1} *
	-	-	-	1.0043×10^{-1} *	1.0186×10^{-1} *
	-	-	-	3.0209×10^{-2} *	2.4008×10^{-2} *
	-	-	-	-	-

$D = \{(x,y): x=a/4, 3a/4; y=b/4, 3b/4\}; (\sigma_{xz}^*, \sigma_{yz}^*, \sigma_{zz}^*):$ computed via constitutive equations

Off-centric localized distributed load

In this last set of analyses a piecewise constant and off-centric loading condition is considered. The distributed load, as depicted in Fig.10, is defined by:

$$\begin{cases} 1, & (x,y) \in \{a/12 \leq x \leq a/4, b/12 \leq y \leq b/4\}; \\ 0, & \text{elsewhere.} \end{cases} \quad (7)$$

Displacements are reported in Table 9. Transverse displacement component, w , is captured more accurately than the in-plane displacement component u . ED4 results for w are practically coincident with those obtained via 3D solution, while w for $a/h=5,2$ is not properly captured. The other 2D theories yield poor results. In Fig.11, u via exact solution, FSDT and

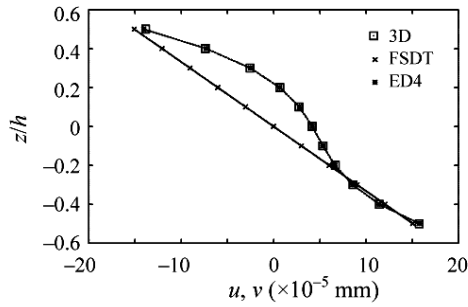


Fig.7 u and v along plate thickness in $(a/4, b/4)$ for localized load, $a/h=2$

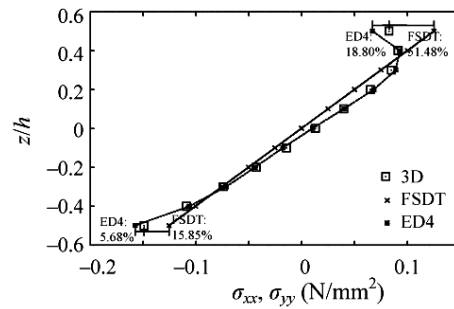


Fig.8 σ_{xx} and σ_{yy} along plate thickness in $(a/4, b/4)$ for localized load, $a/h=2$

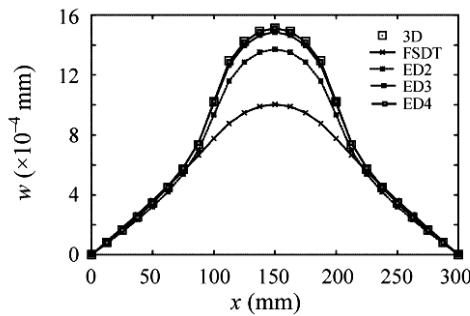


Fig.9 Displacement $w=w(x,b/2)$ at plate top for localized load, $a/h=2$

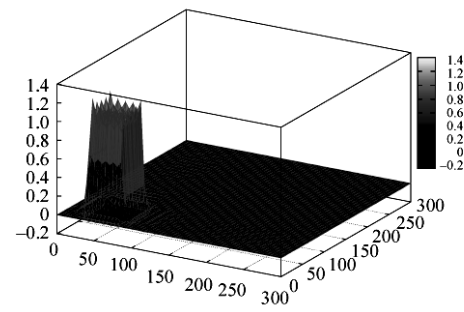


Fig.10 Localized load at $(a/12 \leq x \leq a/4, b/12 \leq y \leq b/4)$ via Fourier's series approximation, $M=N=61$

Table 9 Displacements u, v and w at $(a/4, b/4)$ top for localized load at $(a/12 \leq x \leq a/4, b/12 \leq y \leq b/4)$ (mm)

a/h	u, v, w				
	3D	FSDT	ED2	ED3	ED4
100	-6.4617×10^{-3}	-6.4378×10^{-3}	-6.4792×10^{-3}	-6.4618×10^{-3}	-6.4617×10^{-3}
	-6.4617×10^{-3}	-6.4378×10^{-3}	-6.4792×10^{-3}	-6.4618×10^{-3}	-6.4617×10^{-3}
50	3.848	3.848	3.8473	3.848	3.848
	-1.6320×10^{-3}	-1.6095×10^{-3}	-1.6497×10^{-3}	-1.6322×10^{-3}	-1.6320×10^{-3}
10	-1.6320×10^{-3}	-1.6095×10^{-3}	-1.6497×10^{-3}	-1.6322×10^{-3}	-1.6320×10^{-3}
	4.8245×10^{-1}	4.8291×10^{-1}	4.8211×10^{-1}	4.8245×10^{-1}	4.8245×10^{-1}
5	-7.1240×10^{-5}	-6.4378×10^{-5}	-9.3404×10^{-5}	-7.5497×10^{-5}	-7.2873×10^{-5}
	-7.1240×10^{-5}	-6.4378×10^{-5}	-9.3404×10^{-5}	-7.5497×10^{-5}	-7.2873×10^{-5}
2	4.2612×10^{-3}	4.3209×10^{-3}	4.1924×10^{-3}	4.2606×10^{-3}	4.2613×10^{-3}
	-3.5296×10^{-6}	-1.6095×10^{-5}	-3.2208×10^{-5}	-1.3778×10^{-5}	-8.4254×10^{-6}
2	-3.5296×10^{-6}	-1.6095×10^{-5}	-3.2208×10^{-5}	-1.3778×10^{-5}	-8.4254×10^{-6}
	7.4180×10^{-4}	7.1889×10^{-4}	3.0541×10^{-4}	7.4102×10^{-4}	7.4198×10^{-4}
2	3.6739×10^{-5}	-2.5751×10^{-6}	-6.1265×10^{-6}	4.5108×10^{-6}	1.8869×10^{-5}
	3.6739×10^{-5}	-2.5751×10^{-6}	-6.1265×10^{-6}	4.5108×10^{-6}	1.8869×10^{-5}
2	2.6440×10^{-4}	1.2610×10^{-4}	2.3745×10^{-4}	2.5809×10^{-4}	2.6493×10^{-4}

ED4 are plotted with respect to z for $a/h=10$ in $(a/4, b/4)$. Absolute percentage errors at plate top are 2.29% and 9.63% for ED4 and FSDT respectively. Table 10 presents results on stresses. Higher order theories provide accurate results for σ_{xx} and σ_{yy} even for thick plate regimes, but poor ones for σ_{xy} and σ_{xz} for $a/h=5,2$, indicating that higher polynomial expansion order in

Eq.(2) is required. FSDT for thin plates provides very good results. Fig.12 shows in-plane stress σ_{xx} along the plate thickness for $a/h=2$ via exact model, FSDT and ED4. Absolute percentage error for ED4 model at plate top is 13.8%, while for the rest there is high data accuracy. Transverse displacement $w=w(x,b/4)$ at plate top for a thick plate is reported in Fig.13.

Table 10 In-plane stresses (σ_{xx} , σ_{yy} , σ_{xy}) at ($a/4$, $b/4$) top and out-of-plane stresses (σ_{xz} , σ_{yz} , σ_{zz}) at ($a/4$, $b/4$) middle point for localized load at ($a/12 \leq x \leq a/4$, $b/12 \leq y \leq b/4$) (N/mm²)

a/h	$\sigma_{xx}, \sigma_{yy}, \sigma_{xy}, \sigma_{xz}, \sigma_{yz}, \sigma_{zz}, \sigma_{xz}^*, \sigma_{yz}^*, \sigma_{zz}^*$				
	3D	FSDT	ED2	ED3	ED4
100	1.7098×10^2	1.7091×10^2	1.7095×10^2	1.7101×10^2	1.7098×10^2
	1.7098×10^2	1.7091×10^2	1.7095×10^2	1.7101×10^2	1.7098×10^2
	-3.2160×10^1	-3.2244×10^1	-3.2090×10^1	-3.2159×10^1	-3.2160×10^1
	-3.3530	-3.3568	-3.3568	-3.3533	-3.3530
	-3.3530	-3.3568	-3.3568	-3.3533	-3.3530
	1.2022×10^{-1}	1.2009×10^{-1}	1.2023×10^{-1}	1.2021×10^{-1}	1.2022×10^{-1}
	-	-	-	-3.3507*	-3.3541*
	-	-	-	-3.3507*	-3.3541*
	-	-	-	$1.2021 \times 10^{-1*}$	$1.2022 \times 10^{-1*}$
	-	-	-	-	-
50	4.2796×10^1	4.2727×10^1	4.2765×10^1	4.2828×10^1	4.2796×10^1
	4.2796×10^1	4.2727×10^1	4.2765×10^1	4.2828×10^1	4.2796×10^1
	-8.0013	-8.0610	-7.9255	-7.9970	-8.0010
	-1.6703	-1.6784	-1.6784	-1.6712	-1.6700
	-1.6703	-1.6784	-1.6784	-1.6712	-1.6700
	1.2129×10^{-1}	1.2009×10^{-1}	1.2126×10^{-1}	1.2123×10^{-1}	1.2131×10^{-1}
	-	-	-	-1.6659*	-1.6725*
	-	-	-	-1.6659*	-1.6725*
	-	-	-	$1.2124 \times 10^{-1*}$	$1.2106 \times 10^{-1*}$
	-	-	-	-	-
10	1.7753	1.7091	1.7503	1.813	1.779
	1.7753	1.7091	1.7503	1.813	1.779
	-3.8288×10^{-1}	-3.2244×10^{-1}	-2.5877×10^{-1}	-3.1506×10^{-1}	-3.4317×10^{-1}
	-3.0276×10^{-1}	-3.3568×10^{-1}	-3.3568×10^{-1}	-3.0489×10^{-1}	-2.8778×10^{-1}
	-3.0276×10^{-1}	-3.3568×10^{-1}	-3.3568×10^{-1}	-3.0489×10^{-1}	-2.8778×10^{-1}
	1.2514×10^{-1}	1.2009×10^{-1}	1.2702×10^{-1}	1.2533×10^{-1}	1.2503×10^{-1}
	-	-	-	$-2.8180 \times 10^{-1*}$	$-3.0690 \times 10^{-1*}$
	-	-	-	$-2.8180 \times 10^{-1*}$	$-3.0690 \times 10^{-1*}$
	-	-	-	$1.2469 \times 10^{-1*}$	$1.2510 \times 10^{-1*}$
	-	-	-	-	-
5	5.0123×10^{-1}	4.2727×10^{-1}	4.8577×10^{-1}	5.4277×10^{-1}	5.0461×10^{-1}
	5.0123×10^{-1}	4.2727×10^{-1}	4.8577×10^{-1}	5.4277×10^{-1}	5.0461×10^{-1}
	-1.9713×10^{-1}	-8.0610×10^{-2}	-4.8413×10^{-2}	-8.8136×10^{-2}	-1.1685×10^{-1}
	-1.2817×10^{-1}	-1.6784×10^{-1}	-1.6784×10^{-1}	-1.2669×10^{-1}	-1.0354×10^{-1}
	-1.2817×10^{-1}	-1.6784×10^{-1}	-1.6784×10^{-1}	-1.2669×10^{-1}	-1.0354×10^{-1}
	1.3392×10^{-1}	1.2009×10^{-1}	1.3511×10^{-1}	1.3439×10^{-1}	1.3303×10^{-1}
	-	-	-	$-9.5830 \times 10^{-2*}$	$-1.3356 \times 10^{-1*}$
	-	-	-	$-9.5830 \times 10^{-2*}$	$-1.3356 \times 10^{-1*}$
	-	-	-	$1.3322 \times 10^{-1*}$	$1.3218 \times 10^{-1*}$
	-	-	-	-	-
2	2.1061×10^{-1}	6.8364×10^{-2}	1.8119×10^{-1}	2.5147×10^{-1}	2.3965×10^{-1}
	2.1061×10^{-1}	6.8364×10^{-2}	1.8119×10^{-1}	2.5147×10^{-1}	2.3965×10^{-1}
	-1.6777×10^{-1}	-1.2898×10^{-2}	1.4882×10^{-3}	-7.1998×10^{-3}	-2.9420×10^{-2}
	-2.0627×10^{-2}	-6.7135×10^{-2}	-6.7135×10^{-2}	-1.7173×10^{-2}	1.6681×10^{-2}
	-2.0627×10^{-2}	-6.7135×10^{-2}	-6.7135×10^{-2}	-1.7173×10^{-2}	1.6681×10^{-2}
	9.5365×10^{-2}	1.2009×10^{-1}	1.0546×10^{-1}	9.8474×10^{-2}	9.4399×10^{-2}
	-	-	-	$-2.0298 \times 10^{-2*}$	$-2.7419 \times 10^{-2*}$
	-	-	-	$-2.0298 \times 10^{-2*}$	$-2.7419 \times 10^{-2*}$
	-	-	-	$9.5120 \times 10^{-2*}$	$1.0463 \times 10^{-1*}$
	-	-	-	-	-

($\sigma_{xz}^*, \sigma_{yz}^*, \sigma_{zz}^*$): computed via constitutive equations

CONCLUSION

Closed form exact 3D and 2D plate models have been compared. In the case of 2D theories a hierarchy has been established on the base of the results quality related to the axiomatic assumption of the displacements field. Static analyses of isotropic plates have

been presented taking into account several transverse loading conditions at plate top. Thickness ratio a/h has been chosen as study parameter in order to deal with several types of plates: thin, moderately thick, thick and very thick ones. In the case of bi-sinusoidal loads it has been shown how the accuracy of the results is also influenced by the number of half waves

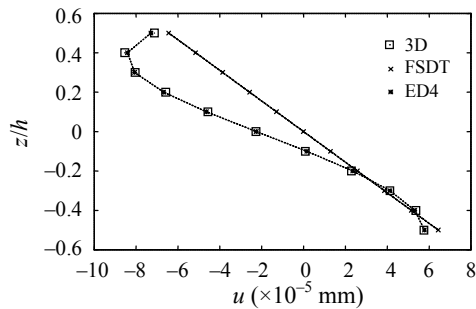


Fig.11 u along plate thickness in $(a/4, b/4)$ for localized load, $a/h=10$

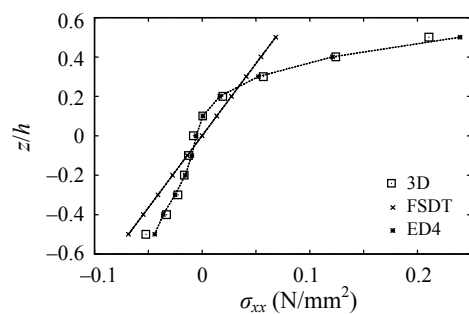


Fig.12 σ_{xx} along plate thickness in $(a/4, b/4)$ for localized load, $a/h=2$

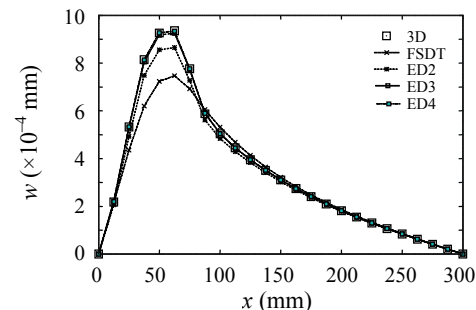


Fig.13 Displacement $w=w(x,b/4)$ at plate top for localized load, $a/h=5$

(m,n) . An explanation has been provided. More general loading conditions have been studied considering a unitary uniformly distributed load and two localized ones: stepwise constant centric and off-centric load conditions. It has been proved that in the case of stepwise constant centric loading conditions higher order 2D models provide highly accurate results for any value of a/h ; FSDT furnishes good accuracy for $a/h \geq 10$. In the case of stepwise constant off-centric load condition and for $a/h \geq 10$ very good results have been obtained by means of higher order 2D models, while for thick ($a/h=5$) and very thick ($a/h=2$) plates a higher expansion order is required.

References

- Anderson, T., Madenci, E., Burton, S.W., Fish, J.C., 1998. Analytical solutions of finite-geometry composites panels under transient surface loadings. *International Journal of Solids and Structures*, **35**(12):1219-1239. [doi:10.1016/S0020-7683(97)82761-8]
- Barrett, K.E., Ellis, S., 1988. An exact theory of elastic plates. *International Journal of Solids and Structures*, **24**(9):859-880. [doi:10.1016/0020-7683(88)90038-8]
- Barut, A., Anderson, T., Madenci, E., Tessler, A., 2000. A Complete Stress Field in Thick Sandwich Construction via Single-layer Theory. Proceeding of the Fifth International Conference on Sandwich Constructions, Zurich, Switzerland, **2**:691-704.
- Carrera, E., 2002. Theories and finite elements for multilayered anisotropic, composite plate and shell. *Archives of Computational Methods in Engineering*, **9**(2):87-140.
- Carrera, E., 2003. Theories and finite elements for multilayered plate and shell: A unified compact formulation with numerical assessment and benchmarking. *Archives of Computational Methods in Engineering*, **10**(3):215-296.
- Carrera, E., Ciuffreda, A., 2005. A unified formulation to assess theories of multilayered plates for various bending problems. *Composite Structures*, **69**(3):271-293. [doi:10.1016/j.compstruct.2004.07.003]
- Carrera, E., Demasi, L., 2003. Two benchmarks to assess two-dimensional theories of sandwich, composite plates. *AIAA Journal*, **10**(41):1356-1362.
- Demasi, L., 2007. Three-dimensional closed form solutions and exact thin plate theories for isotropic plates. *Composite Structures*, **80**(2):183-195. [doi:10.1016/j.compstruct.2006.04.073]
- He, J.F., 1995. A twelfth-order theory of antisymmetric bending of isotropic plates. *Int. J. Mech. Sci.*, **38**(1):41-57. [doi:10.1016/0020-7403(95)00034-U]
- Levinson, M., 1985. The simple supported rectangular plate: an exact, three-dimensional, linear elasticity solution. *Journal of Elasticity*, **15**(3):283-291. [doi:10.1007/BF00041426]
- Love, A.E.H., 1944. *A Treatise on Mathematical Theory of Elasticity*. Dover, New York.
- Meyer-Piening, H.R., 2000. Experiences with 'Exact' Linear Sandwich Beam and Plate Analyses Regarding Bending, Instability and Frequency Investigation. Proceeding of the Fifth International Conference on Sandwich Constructions, Zurich, Switzerland, **1**:37-48.
- Pagano, N.J., 1969. Exact solution for composites laminates in cylindrical bending. *Journal of Composite Materials*, **3**(3):398-411. [doi:10.1177/002199836900300304]
- Pagano, N.J., 1970. Exact solution for rectangular bidirectional composite and sandwich plates. *Journal of Composite Materials*, **4**(1):20-34. [doi:10.1177/002199837000400102]
- Reddy, J.N., 1997. *Mechanics of Laminated Composites Plates: Theory and Analysis*. CRC Press, Boca Raton, Florida.
- Timoshenko, S., Woinowsky-Krieger, S., 1959. *Theory of Plates and Shells*. McGray-Hill, New York.
- Zenkour, A.M., 2003. An exact solution for the bending of thin rectangular plates with uniform, linear and quadratic thickness variations. *Int. J. Mech. Sci.*, **45**(2):295-315. [doi:10.1016/S0020-7403(03)00050-X]